Published in the Proceedings of the 16th International Aluminum Alloys Conference (ICAA16) 2018
ISBN: 978-1-926872-41-4
by the Canadian Institute of Mining, Metallurgy & Petroleum

EFFECT OF CUBE TEXTURE ON THE PLANAR ANISOTROPY IN A NOVEL Al-Mg-Si-Zn ALLOY

*Zhenshan Liu[1,2,a], Pizhi Zhao[1,2,b] , Yiheng Cao[1,2,c] and Jingwei Zhao[1,2,c]

[1] *Chinalco Material Applications Research Institute Co.LTD*
Future Science and Technology Park, Changing District, 102209 Beijing China
*(*Corresponding author:zhenshan.liu@outlook.com)*

[2] *Chinalco Research Institute of Science and Technology*
Future Science and Technology Park, Changing District, 102209 Beijing China

ABSTRACT

A new Al-Mg-Si-Zn alloy designed for automotive outer panel was trial-produced with industrial procedure. The final product shows a strong planar anisotropy. X ray diffraction analysis shows such strong anisotropy is caused by the dominating cube texture component in the final product. The reason for such high cube texture component was investigated by tracing texture evolution starting from the hot roll slab. It is found that certain cube texture components already exists in the hot rolled slab. The density of cube texture component shows as a wavy change through the following 1st cold rolling, inter-annealing, 2nd cold rolling and solution treatment. This study shows that the cold rolling in the laboratory can well represent the texture evolution during the industrial production. The results obtained by lab rolling hints that change of second cold rolling reduction has weak effect on the planar anisotropy, when the gauge of hot rolled slab and final sheet are fixed.

KEYWORDS

Aluminum alloys, Texture, Anisotropy, Annealing, Rolling reduction

INTRODUCTION

With the rapid progress of light-weighting in the automotive industry, aluminum sheets get more and more application as closure panel and structure parts. Recently the dominating alloy for outer panel is 6xxx series, containing the main alloy elements Mg and Si. The popular grades are AA6016, AA6111, AA6022, and AA6014. These alloys still cannot satisfy the various requirements from automotive manufacturers. Most suppliers of automotive aluminum sheets are developing their own specific grades according to the customer's demand. To increase the baking response, a new Al-Mg-Si-Zn alloy was designed, concerning the high combination energy between Zn solutes and vacancies formed during the quenching stage of automotive sheet manufacture. This combination is helpful to the precipitation of β" phase during the paint baking (Wang, 2015, 2016; Yan, 2014).

The plastic strain ratio (r value) is a key index of the formability of automotive body sheet. A high r value means a good formability. The r values in different directions can be used to evaluate the planar anisotropy of the metal sheets. The trial produced Al-Mg-Si-Zn sheet shows a strong planar anisotropy with respect to r values. Since the r value is tightly related with texture, the texture evolution from hot roll slab (HRS) to final T4P temper was analyzed with X ray diffraction (XRD) to find the reason for the high anisotropy. Besides, the cold rolling reduction (CRR) was varied in the laboratory to modify the texture distribution, i.e., the planar anisotropy.

EXPERIMENTAL

The investigated Al-Mg-Si-Zn sheet was produced by Southwest Aluminum (Group) Co., Ltd. The chemical composition range is given in Table 1. The HRS was cold rolled from 5.7 mm to 3.2 mm firstly. The 1st cold rolled sheet is denoted as CR1. Then it was inter-annealed at the temperature of 420℃ for 2 hours, denoted as AIA. With the 2nd cold rolling the gauge reached 0.98 mm, i.e., 2nd CRR is 70%. This sheet is denoted as CR2. After following solution treatment at the temperature of 545℃ with continuous annealing line, the sheet was water quenched. The consequent T4P was given by pre-aging. For convenience to refer, the sheet fabricated in plant is named as "plant 70%".

Table 1. Chemical composition range of investigated alloys (mass, %)

Si	Fe	Cu	Mn	Mg	Zn	Zr
0.8~1.1	0.05~0.20	0.1~0.3	0.05~0.20	0.4~0.7	0.5~0.7	0.02~0.10

To study the influence of 2nd CRR on the texture and the r value, the HRS produced in the plant was cold rolled to various thicknesses in the laboratory. These cold rolled sheet was inter-annealed with the same procedure in plant (at 420°C for 2 hours), and then 2nd cold rolled to 0.98 mm. In present work the sheets were prepared with 2nd CRR of 60, 70, 80%. These sheets were solution annealed at the temperature of 545°C with salt bath. T4P was given by pre-aging. Also for referring convenience, these sheets with 2nd CRR of 60, 70, 80% are named "lab 60%", "lab 70%", and "lab 80%", respectively.

Tensile tests were performed with SHIMADZU AG-xplus100kN. The gauge length of tensile specimens is 50 mm. Specimens was first tensioned with a slow speed of 3 mm/min, then 24 mm/min after yielding point. The r-values were calculated with strain along the transvers direction and through-thickness strain. Specimens with angles of 0°, 45°, and 90° between the tensile direction and rolling direction were tested respectively. For each direction, three specimens were analyzed.

Specimens for optical metallography were ground, polished, and anodized with mixed acid solution (H_2SO_4: H_3PO_3:H_2O=38:43:19) for grain size measurement. The specimens for secondary phase observation was etched with 0.5% HF acid for 5-10 s. Secondary phase were observed with SEM (JEOL JSM-7800F) under the back scatter model. The textures were obtained with PANalytical X'Pert X-ray diffractometer by the Schulz back reflection method. The measurement was conducted in the ND surface of the sheet for the macro-texture analysis. From the three pole figures ({111}, {200} and {220}) the three dimensional orientation distribution functions (ODF) were calculated with software X'Pert Texture.

RESULTS

Mechanical Properties

Specimens fabricated in plant (plant 70%) and prepared in lab were tested in T4P temper. Table 2 shows that the yield strength of specimens from plant is roughly 10MPa higher than lab prepared. The reason is that samples from suffered a tension levelling to achieve a good flatness, while the lab prepared samples jumped this step.

Table 2. Mechanical properties of sheet from plant and samples prepared in the laboratory

ID	Direction (°)	R_m (MPa)	$R_{p0.2}$ (MPa)	A_{50} (%)	$n_{10\sim20}$	r_{10}	**Δr**
plant 70%	0	270	156	28	0.25	0.93	
plant 70%	45	262	151	27	0.26	0.38	0.39
plant 70%	90	258	148	26	0.26	0.60	
lab 60%	0	270	144	27	0.28	0.91	
lab 60%	45	271	142	31	0.30	0.38	0.46
lab 60%	90	262	139	29	0.30	0.76	
lab 70%	0	275	147	27	0.28	0.91	
lab 70%	45	268	141	32	0.30	0.36	0.50
lab 70%	90	262	140	28	0.30	0.80	
lab 80%	0	271	145	27	0.28	0.90	
lab 80%	45	266	142	32	0.30	0.33	0.48
lab 80%	90	264	143	28	0.30	0.71	

Both the yield strength and r value in 0°, 45°, 90° direction hint at a strong anisotropy of the new Al-Mg-Si-Zn sheet (Figure 1). The yield strength along tensile direction is larger than that perpendicular to rolling direction, with increasing of CRR the difference becomes smaller. The r values in three directions look like a V shape, the values in 0° and 45° are quite close to each other for different specimens, but 90° direction shows a large scatter. The sample plant 70% shows the minimum Δr, although owning the same CRR, the sample lab 70% has the maximum Δr. No linear correlation is observed between CRR and Δr.

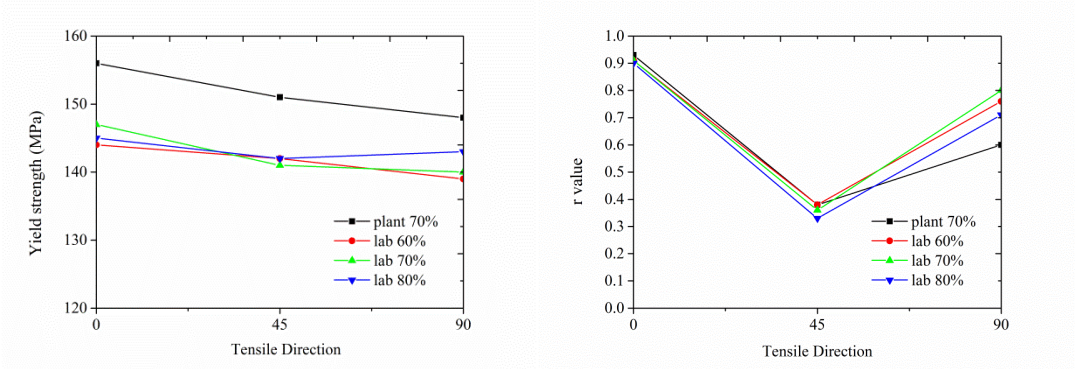

Figure 1. Yield strength and r value of specimens from plant trial (plant 70%) and lab prepared with 2nd CRR of 60, 70, 80% (lab 60%, lab 70%, lab 80%)

Microstructural Features

Figure 2 demonstrates the grain structure evolution of the sheet fabricated in plant. Elongated fiber in the HRS becomes much finer after 1st cold rolling. During the inter-annealing, the recrystallization happens, coarse elongated grain is observed. After 2nd cold rolling and solution treatment, these large grain become fine. The grain sizes along RD, ND, and TD are 44, 30, 41 μm, respectively.

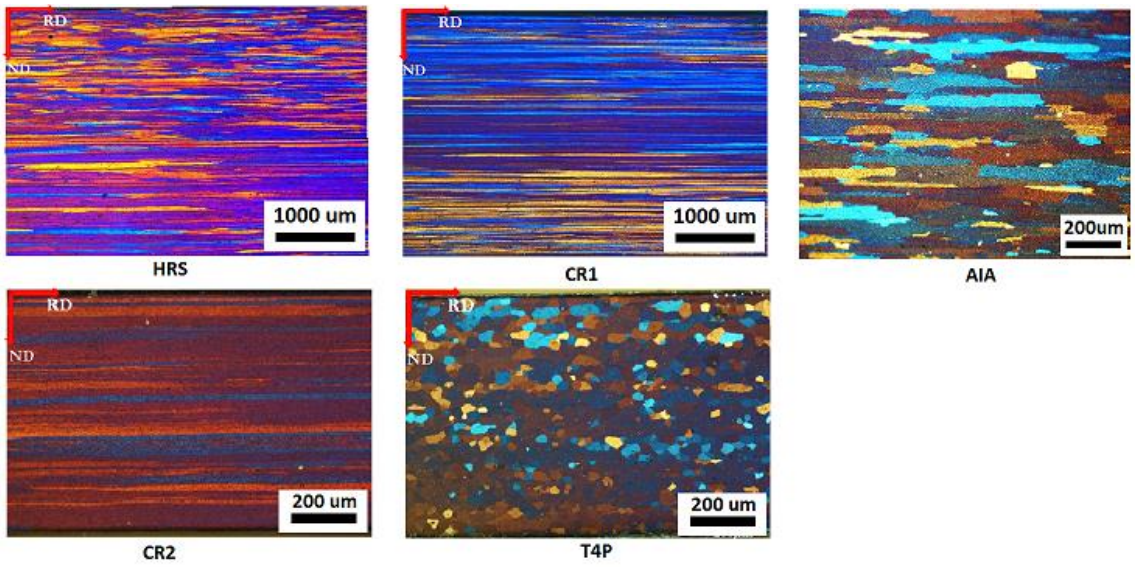

Figure 2. Optical micrographs of Al-Mg-Si-Zn sheet after different processing stages in plant

T4P samples prepared in the lab show also equiaxed recrystallization structure (Figure 3). The grain sizes decrease with CRR (60, 70, 80%), along RD are 40, 35, 33 μm, along ND are 28, 25, 23 μm.

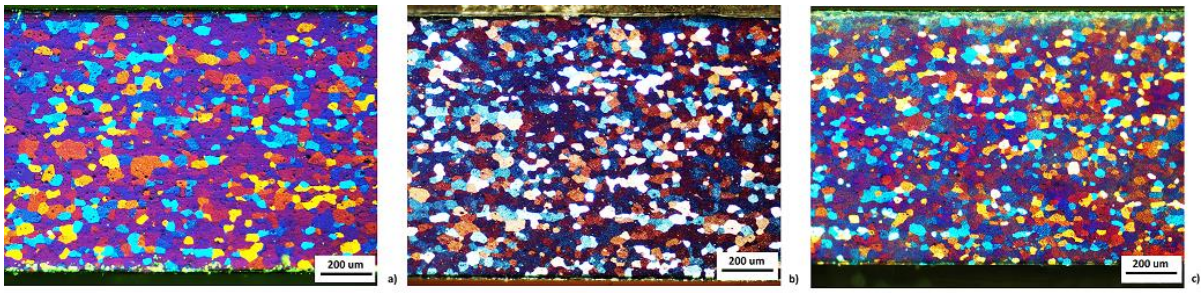

Figure 3. Optical micrographs of lab prepared specimens (T4P) with 2nd CRR of 60, 70, 80% (TD plane)

Secondary Phase

Figure 4 illuminates the evolution of secondary phase during different producing stages in plant. In the HRS the iron bearing particles are dominating, only rare coarse Mg_2Si constituent is observed (Figure 5), which is formed during casting (Yan 2014). No variation happens during 1st cold rolling. It is worth to notice that during the inter-annealing plenty of fine dark dispersoids form. Meanwhile the amount of preexisted iron bearing particles increases. Similar to 1st cold rolling, nothing occurs during 2nd cold rolling with respect to secondary phase. During the following solid solution treatment, most of these dark dispersiods dissolve, which promises a good baking response.

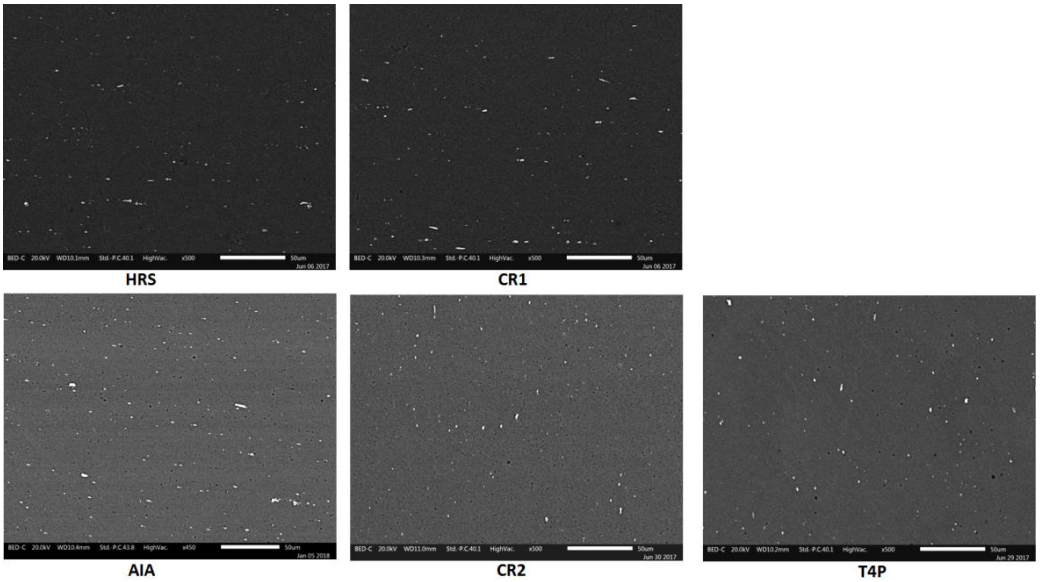

Figure 4. Secondary phase in Al-Mg-Si-Zn sheet after different processing stages in plant

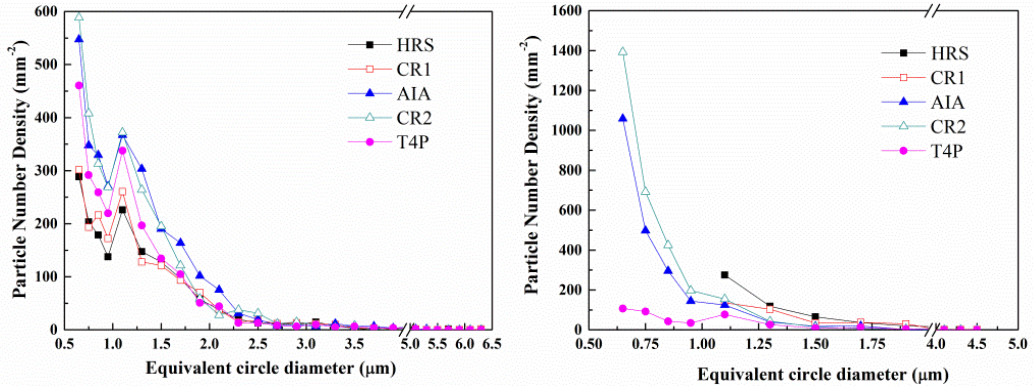

Figure 5. Secondary phase evolution from HRS to T4P temper, a) iron bearing particle, b) dark Mg_2Si particles in Figure 4

Texture Evolution

All ODF calculations were performed under the assumption of orthotropic sample symmetry as defined by the rolling direction, the transverse direction, and the normal direction of the rolled sheets, demonstrated as Figure 6. From the ODF figure, orientation densities f(g) was extracted for comparison.

Figure 7 gives the orientation densities along the β-fiber versus the corresponding Euler angle φ_2. The HRS shows a combination of deformation and recrystallization texture. The density of deformation texture components is smooth along the β-fiber in the range from 5 to 10, meanwhile the density of cube texture component is as high as 15. The 1st cold rolling makes the S texture component increase intensively. During the inter-annealing the recrystallization texture becomes dominating (Figure 8), and deformation texture almost disappears. Although the 2nd CRR is larger than the 1st CRR, the densities of deformation texture after 2nd cold rolling is much lower than that after 1st cold rolling. Some amount of cube texture still preexist after 2nd cold rolling (Figure 8). Following solid solution treatment leads to much higher cube texture component.

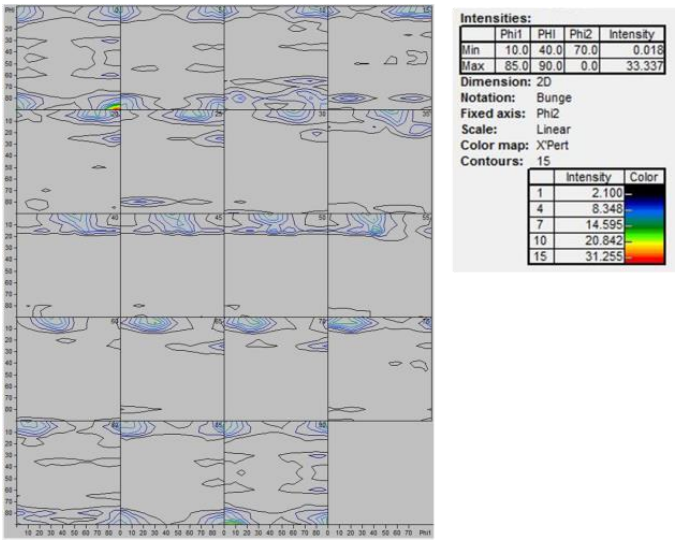

Figure 6. Texture of T4P temper sheet fabricated in plant

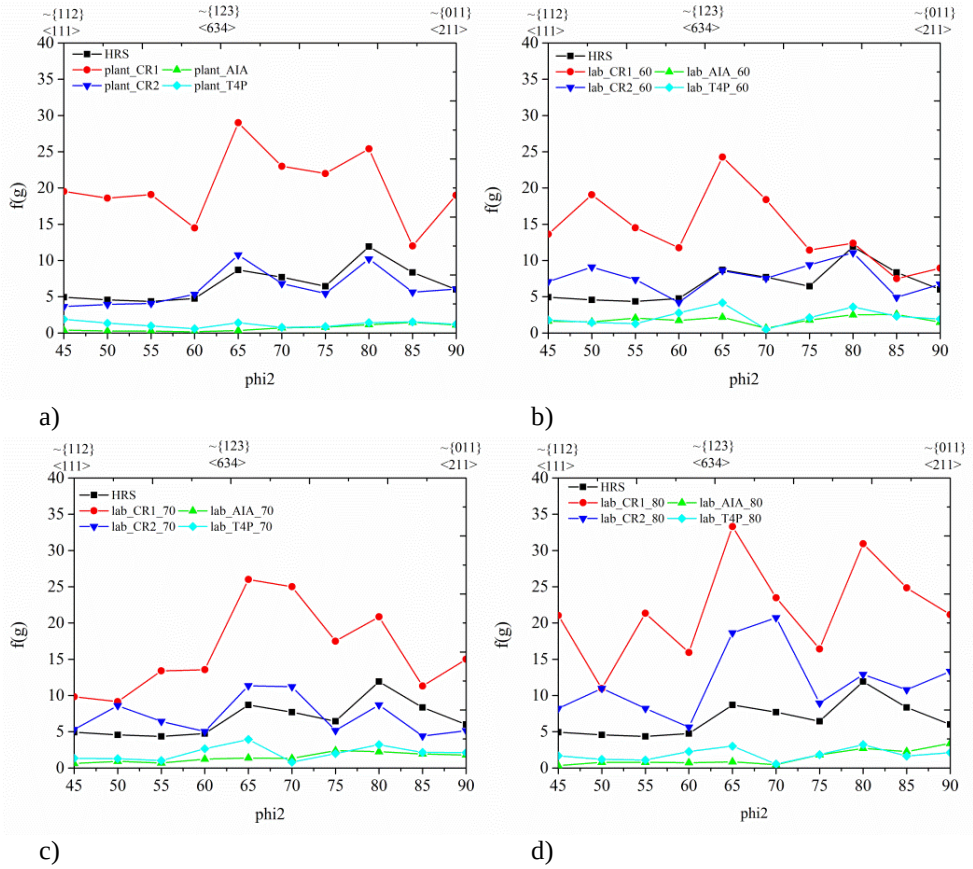

Figure 7. Texture evolution from HRS to T4P temper, a) plant manufactured with 2nd CRR of 70%, b)-d) lab prepared with2nd CRR of 60%, 70%, 80% respectively

DISCUSSION

Comparison Between Plant 70% and Lab 70%

Although the CRRs of sample plant 70% and lab 70% are the same with each other, there are still some differences during the processing. Firstly the rolling speed in the plant is much higher than that in the lab. Secondly the solid solution in plant was performed with continuous air cushion furnace, in contrast, salt bath is used for solid solution treatment. Thirdly the pre-aging step in plant was realized by heating and storage in the air, which is totally different with in the lab (70°C for 7 hours). However, these differences do not lead to essential difference of microstructure between sample plant 70% and lab 70%. Figure 2 and Figure 3 illustrate that their grain structure at T4P temper are similar, only 5 μm difference. Figure 7 a), c) and Figure 8 show the texture evolution from HRS to T4P for both cases have the same tendency. Therefore, it is concluded that the lab procedure can represent the industrial manufacture procedure with respect to texture evolution.

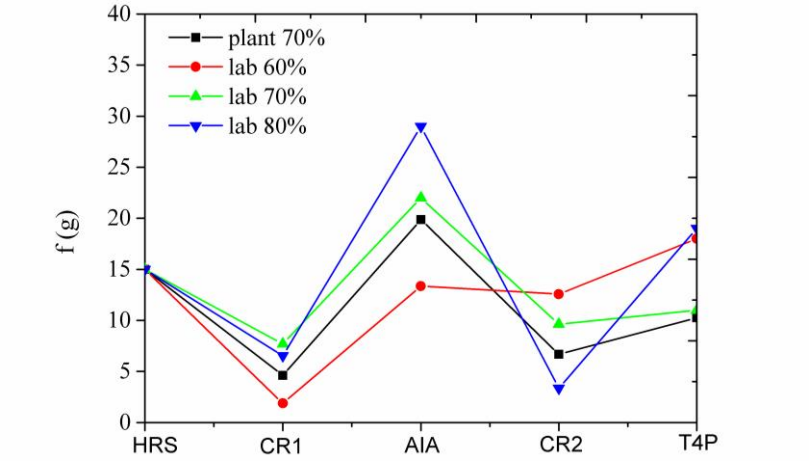

Figure 8. Cube texture component evolution from HRS to T4P temper with various CRR

Influence of CRR on Texture Evolution

As shown in Figure 7 and 8, the texture component distributions at T4P temper are quite close to each other despite of different CRR. Density along β fiber is 2–3. The density of cube texture with CRR 60% and 80% are the same with each other. This agrees well with the relationship between r value and CRR (Figure 1).

Apparently the texture distribution has no or weak relationship with CRR, indeed CRR has a strong influence on texture evolution, when man traces the texture from HRS. In Figure 8, we find the cube texture density of HRS decreases after the 1st cold rolling. In our case the HRS gauge and final sheet (T4P) gauge are fixed, larger 2nd CRR means smaller 1st CRR. Hence, sample lab 80% with smallest 1st CRR keeps the highest cube texture density from HRS. During the following inter-annealing, its cube texture increases rapidly, because the remaining grains with cube orientation serve as recrystallization nuclei. At the CR2 step, the high 2nd CRR makes its cube texture drops dramatically. In the following solid solution the cube texture cannot reach as high fraction as AIA.

Texture evolution of sample lab 60% goes through another routine. Higher 1st CRR reduces the remaining cube texture from HRS, which serves as nuclei of recrystallization. Hence less cube texture component forms after inter-annealing. Low 2nd CRR only reduces the cube texture slightly during the CR2, however, low 2nd CRR means low recrystallization driving force, cube texture only increase smoothly during solid solution treatment.

CONCLUSIONS

In present work the mechanical properties and texture evolution of new Al-Mg-Si-Zn alloy was investigated. The strong planar anisotropy of new Al-Mg-Si-Zn alloy is caused by high cube texture component in T4P temper. Such high cube texture component origins from the cube texture components already existed in the hot rolled slab.

By comparison between sample plant 70% and lab 70%, it is concluded that the cold rolling in the laboratory can well represent the texture evolution during the industrial production. With lab rolling, it is found that change of second cold rolling reduction has weak effect on the planar anisotropy, when the gauge of hot rolled slab and final sheet are fixed.

ACKNOWLEDGMENTS

This work was supported by the National Key Research and Development Plan (project No. 2016YFB0300800). Many thanks are extended to all colleagues and co-workers in this projects for their excellent collaboration.

REFERENCES

Engler, O., Hirsch, J., (2002). Texture control by thermomechanical processing of AA6xxx Al-Mg-Si sheet alloys for automotive applications—a review. *Materials Science and Engineering A, 336*, 249–262. https://doi.org/10.1016/S0921-5093(01)01968-2

Randle, V., & Engler, O. (2000). *Introduction to texture analysis: macrotexture, microtexture and orientation mapping*. Amsterdam: Gordon and Breach Science Publishers.

Tian, N., Zhao, G., Nie B., Wang, J.J., & Zuo, L. (2012). Texture and correlation between R-value and formability of aluminum alloy sheet. *Materials Science Forum, 702–703*, 356–359. https://doi.org/10.4028/www.scientific.net/MSF.702-703.356

Wang, X.F, Guo, M.X., Chapuis, A., Luo, J.R., Zhang, J.S., & Zhuang, L.Z. (2015). Effect of solution timeon microstructure, texture and mechanical properties of Al–Mg–Si–Cu alloys. *Materials Science and Engineering: A, 644*, 137–151. https://doi.org/10.1016/j.msea.2015.07.059

Wang, X.F, Guo, M.X., Zhang, J.S., & Zhuang, L.Z. (2016). Effect of Zn addition on the microstructure, texture evolution and mechanical properties of Al-Mg-Si-Cu alloys. *Materials Science and Engineering: A, 677*, 522–533. https://doi.org/10.1016/j.msea.2016.09.084

Yan, L.Z., Zhang, Y.A., Li, X.W., Li. Z.H., Wang, F., Liu, H.W., & Xiong, B.Q. (2014). Microstructural evolution of Al–0.66Mg–0.85Si alloy during homogenization, *Transactions of Nonferrous Metals Society of China*, *24*(4), 939–945. https://doi.org/10.1016/S1003-6326(14)63146-0